

Proceedings of the Institute of Acoustics

PHOTOACOUSTIC EXAMINATION OF SELECTED MATERIALS

(a review)

A. Śliwinski

Institute of Experimental Physics, University of Gdansk,
80-952 Gdansk, Poland

1. INTRODUCTION

In a very wide range of interest of Dr R.W.B. Stephens the photoacoustic effect presented a peculiar role during last decade of his life. At the First Spring School on Acoustooptics and its Applications (Gdansk-Wiezyca, 1980) he read the invited paper [1] reviewing the state of the art of that topic in the theory and in experiment as well. The photoacoustic spectroscopy (PAS) principles based on the Rosencwaig and Gersho [2], Aamodt, Murphy and Parker [3] theories as well as the generalized Mc Donald and Wetsel [4] theory were fully described in his lecture supported by some original results of measurements performed in the Chelsea College, London. Since that time the interest in that kind of spectroscopy has been strongly developed over the world [5,6] and the R.W.B. Stephens' lecture in Gdansk in 1980 initiated PAS research in our University and several other places in Poland [7].

In this paper some results obtained by our group of co-workers at the Department of Applied Physics of the University of Gdansk are reviewed. Photoacoustic measurements were performed in different materials which also were examined by other spectroscopic methods. Below, some results for three kinds of materials are described, namely, Europium Chelate Powder (A. Sikorska, S. Zachara [8]), Rodamine 6G in PVA foil (J. Szurkowski) and plant leaves influenced by tumor (Cz. Lewa [9], J. Szurkowski, G. Zebrowska [10]). The photoacoustic spectra were obtained using the photoacoustic spectrometer set down in our lab. The other spectra were got by conventional spectrometers. Photoacoustic spectra are presented and discussed in comparison to absorption and excitation ones (in the case of Europium Chelate and rodamine 6G). In the case of plant leaves the photoacoustic spectra were obtained for healthy leaves and the ones with crown gall tumors and compared.

2. EXPERIMENTAL SETUP

The photoacoustic spectrometer was set down according to the scheme presented in the Fig.1. The Xenon Lamp XHP 150 was used as a source of light S. The light beam was focused on the slit of the grating monochromator M (SPM 2), passed through it and was modulated with a mechanical chopper C; next focused by the lense L (and directed with the mirror Z) on the sample situated in the photoacoustic cell K. The photoacoustic signal created in the cell was detected with the microphone M (Bruel & Kjaer - typ 4146) preamplifier W and the lock-in amplifier V (UNIPAN - type 232 B) controlled by the reference signal picked up with the phototransistor situated

PHOTOACOUSTIC EXAMINATION ...

behind of the chopper C. The output signal was recorded and stored for processing by the system controller N (Neptun 184 microcomputer) synchronously turning the grating of the monochromator with the motor E. The data were sampling every 1 nm and the spectrum read out rate was 10 nm/min.; the spectral width at the output of the monochromator was 10 nm. The modulation frequency could be chosen from 10 to 30 Hz.

According to the theory [2,3] the amplitude of a photoacoustic signal may be expressed in the following way:

$$s(\lambda) = k I_0(\lambda) \beta(\lambda) \alpha(\lambda), \quad (1)$$

where $s(\lambda)$ is the amplitude of the signal component for a given wavelength λ for the incidenting the sample light intensity $I_0(\lambda)$; $\beta(\lambda)$ is the light absorption coefficient, $\alpha(\lambda)$ is a part of the energy absorbed and transferred into heat, k is a constant depended on thermal properties of the sample, the photoacoustic cell characteristic and the detection system.

In a case when the absorption of light of the wave-length λ was associated with the emission of various wavelength λ_i having quantum efficiencies η_i , the expression (1) is written as [12]:

$$s(\lambda) = k I_0(\lambda) \beta(\lambda) \left(1 - \sum_{i=1}^n \eta_i \frac{\lambda}{\lambda_i} \right). \quad (2)$$

Usually, the photoacoustic signal is normalized to the reference signal $R(\lambda) = k^* I(\lambda)$ obtained from the reference sample for which the absorption coefficient does not depend on the wave-length what leads to the independence of the signal from the light source spectral distribution $I_0(\lambda)$. Then, the relative signal for a sample examined depends only on its optical and thermal properties:

$$S(\lambda) = \frac{s(\lambda)}{R(\lambda)} = k^* \beta(\lambda) \left(1 - \sum_{i=1}^n \eta_i \frac{\lambda}{\lambda_i} \right), \quad (3)$$

where

$$k^* = \frac{k}{k^*}.$$

The photoacoustic spectroscopy [5,6] provides a possibility to examine the depth profile of a sample by alternating the modulation frequency of the incident light. This is related to the fact that the photoacoustic signal is created only by the heat generated within one thermal diffusion length $\mu = (\alpha f)^{-1/2}$ beneath the sample surface, where α is the thermal diffusivity and f the modulation frequency of the incident light beam.

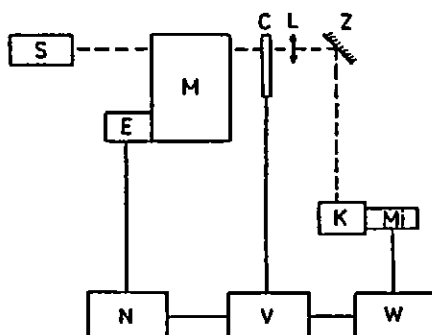


Fig.1

3. PHOTOACOUSTIC STUDIES ON EUROPIUM CHELATE POWDER (A.Sikorska, S.Zachara).

The substance examined was the four ligand complex compound i.e. $\text{Eu}(\text{DBM})_3\text{HP}$, where DBM is dibenzoylmethane, P-pipridine. According to [11] the organic part and the Europium ion may be treated as weakly interacting centres separately for absorption and separately for emission with possible unidirectional energy transfer from the ligand to the ion.

The photoacoustic spectroscopy provides direct information about non-radiative relaxation processes so, applying the method one could expect a way to recognize energy distribution mechanisms occurring in the compound under investigation.

The scheme of energy levels in the chelate is presented in the Fig.2. There are two centres: of absorption in the ligand and of emission in the ion. S_0 represents the ground state of the molecule, S_1 the first excited singlet state of the ligand, T_1 the lowest triplet level of the ligand, 3D_J ($J = 0, 1, \dots$) are sub-levels of the excited Eu^{3+} , 7F_J ($J = 0, 1, \dots$) - sub-levels of the ground state of Eu^{3+} . The arrows correspond to radiative transfers (—) and non-radiative ones (---), respectively.

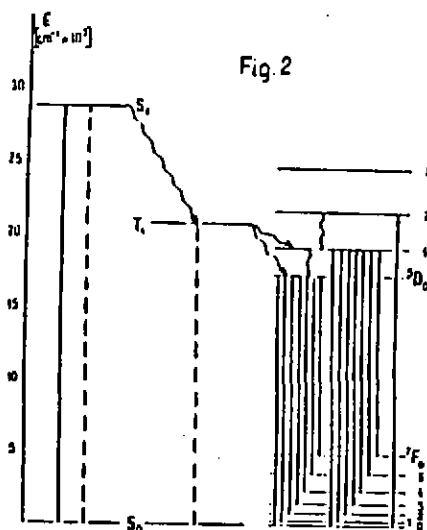


Fig.2

The measurements were performed in room temperature. Before situating in the cell the polycrystalline samples were pulverized and mixed with SiO_2 to get the optical dilution. The PA spectra of a given sample were every time calibrated in respect to the carbone powder reference.

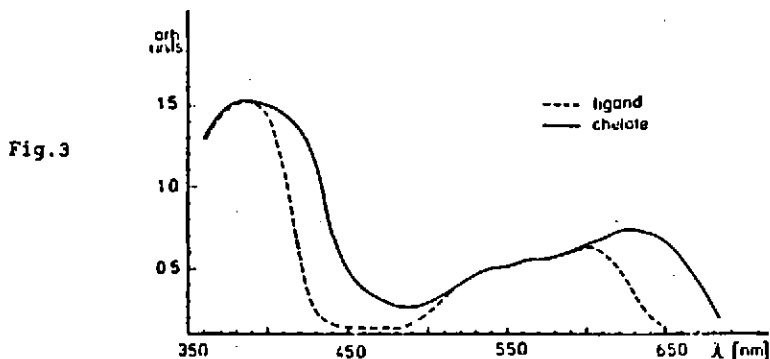


Fig.3

PHOTOACOUSTIC EXAMINATION ...

In the Fig.3 the PA spectra for the chelate and for the dibenzoylmethane (ligand) are presented, respectively. Both spectra have two characteristic bands with that the spectrum of chelate is evidently broadened from the long wave side.

The Fig.4 represents the excitation spectrum recorded for the wave-length 705 nm.

In the excitation spectrum except the evident maximum at 410 nm some weak maxima appear at 460 nm and 525 nm.

The absorption spectrum (Fig.5) obtained for the chelate solution in methanol has the strong, wide maximum at 370 nm and the very weak rest absorption in the long wave side rapidly disappearing at 700 nm.

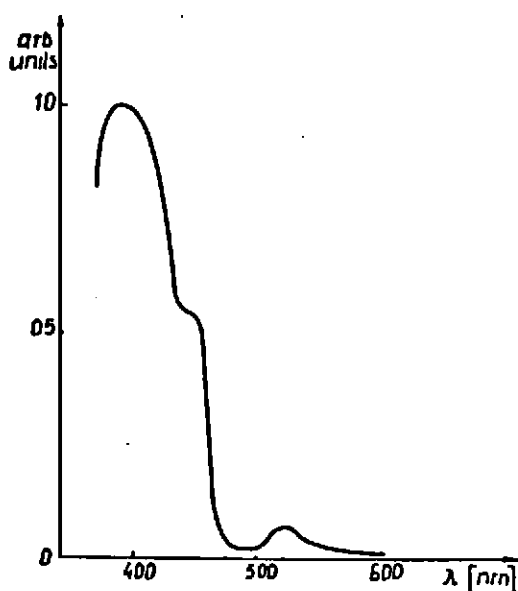


Fig.4

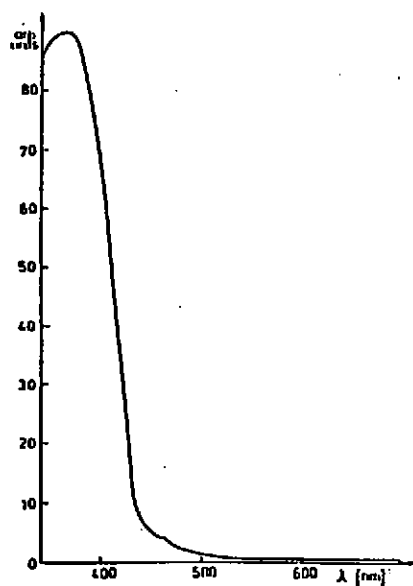


Fig.5

The main condition for the generation of photoacoustic and excitation spectra is the absorption of light by the sample. According to the formula (1) the photoacoustic signal is proportional to the amount of energy transformed into heat. Instead, the excitation spectrum informs about the part of energy being radiated.

The comparison of the both spectra with the absorption one of the che-

late in the solution leads to the following conclusions:

1. The absorption of energy mainly takes place in the organic part of the complex (the short wave band in the Figs 3,4 and 5 corresponds to the transition $S_0 \rightarrow S_1$ shown in the Fig.1).

2. Also, there is absorption directly from the ground level 3F_0 to the levels 3D_2 and 3D_1 (the maxima at 460 nm in the Figs 4 and 5 and at 525 nm in the Fig.4).

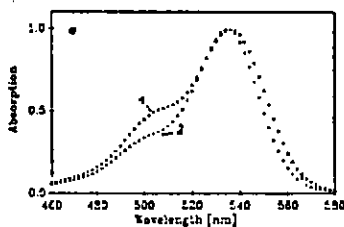
3. The thermal deactivation efficiency after the light absorption by the organic part of the chelate is small (a small height of the "blue" maximum of the PS signal (Fig.3) in comparison to the height of that maximum in the absorption spectrum (Fig.5).

4. The thermal deactivation efficiency within the band 500-700 nm is very great. Interpretation of that phenomenon presents many difficulties, also, for other metals of rare earths [12,13].

4. PHOTOACOUSTIC PROPERTIES OF DIMERS OF 6G RODAMINE IN THE POLYVINILE ALCOHOLE (PVA)

(J.Szurkowski)

Spectral properties of dyes solutions depend on the concentration. Increasing the concentration of a solution one can observe variations (in different kind of spectra) related to the structural association of molecules as appearing of dimers in the solution, for instance.



Such variations of the spectral properties of rodamine 6G in PVA against concentration of rodamine from $6.3 \cdot 10^{-4}$ M to 10^{-3} M are presented. They were examined for different thickness of samples from 0.05 mm to 0.29 mm measuring absorption, photoacoustic and fluorescent excitation spectra, respectively.

In the Fig.6 a,b,c as an example of results the three kinds of spectra (i.e. absorption (a), PAS (b) and fluorescent excitation (c)) are presented for comparison. The samples had the thickness of 0.05 mm and optical density below 0.1 what corresponded to the case of optically and thermally thin samples. According to the theory [2] photoacoustic spectra

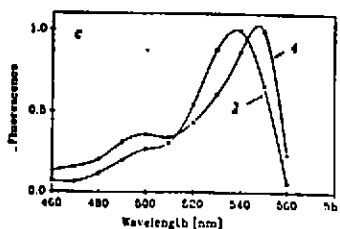
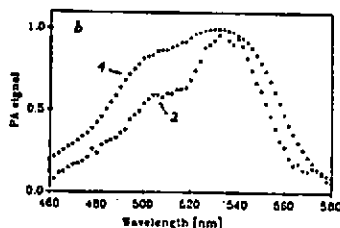


Fig 6

PHOTOACOUSTIC EXAMINATION ...

of such samples can be described by

$$S(\lambda) \sim \epsilon c l (1 - \eta), \quad (4)$$

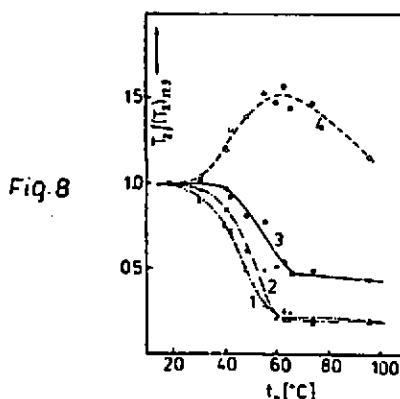
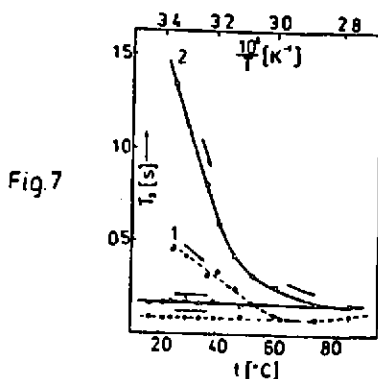
where ϵ is the absorption coefficient, c - concentration, l - thickness and η - fluorescent efficiency.

For lower concentrations (curve 1, $C = 10^{-3}$ M) the absorption as well as the photoacoustic spectra are characteristic for the monomer form of rodamine 6G molecules, however for greater concentrations (curve 2, $C = 10^{-1}$ M) they are changed showing appearing of rodamine 6G dimers in the solution. One can observe that the absorption spectrum is less changed than the photoacoustic and the fluorescent excitation ones. This can be explained by the greater thermal deactivation of dimers than of monomers.

The photoacoustic spectra are more sensitive for aggregation than the absorption ones. The photoacoustic spectrum for that sample is shifted towards the short wave side and the fluorescent excitation spectrum towards the long wave side in respect to the absorption spectrum.

5. PHOTOACOUSTIC SPECTRA OF CROWN GALL TUMORS IN LEAVES OF KALANCHOE DAIGREMONTIANA (Cz.Lewa, J.Szurkowski, G.Żebrowska)

Interesting results were obtained by Cz.Lewa and M.Lewa [9] for temperature dependence of proton nuclear magnetic resonance (NMR) relaxation time T_1 for intact and neoplastic tissues. The Fig.7 represents an example of such a dependence of T_1 for normal (1) and tumorous (2) tissues collec-



ted from kalus culture *Nicotiana Tabacum* (NT) showing evident differentiation. Another dependence of relative value of T_1 in respect to the temperature of 17.5°C as a function of temperature of heating is presented in the Fig.8 for normal kalus NT (1), tumor kalus NT (2), interstitial sites of plant KD (*Kalanchoe daigremontiana*) (3) and leaves of plant KD (4).

PHOTOACOUSTIC EXAMINATION ...

These results stimulated further examinations, [14] also using the PAS method [10]. The mature KD leaves with crown gall tumors initiated by *Agrobacterium tumefaciens* and intact (healthy) leaves were used for PAS experiments. The leaves about 15 mm long were cut in small sections and placed in the photoacoustic spectrometer. Measurements were carried out with the upper epidermis of the leaf facing the light. The samples exhibited no signs of damage, even after prolonged measurements.

The Fig.9 represents the PAS records at frequency 18 Hz for tumorous (●) and healthy (▲) leaf, respectively. The PA signal for tumorous leaf is stronger than that of the intact one. Also, the characteristic maximum is shifted from 545 to 526 nm in the spectrum of tumorous tissue. The frequency response corresponds to a thermal diffusion length of 42 μm while the green (mesophyll) layer of KD leaves begins at the depth of about 50 μm . The PAS of a green leaf resembles the reflectance spectrum [15] with the maximum at 545 nm (Fig.9). This indicates that the PAS is mainly determined by scattered green light from deeper layers which may have been unspecifically absorbed in the epidermis. In the case of tumour tissue the structure of the upper layer of the epidermis is changed and thus a shape of the PAS spectrum is not already determined by the absorption of scattered light but rather by absorption of pigments incorporated in epidermis. The PA signal increases below 450 nm what may occur due to light absorption by flavanoids present in vacuoles of the epidermis cells.

The Fig.10 presents the PA signal against light modulation frequency

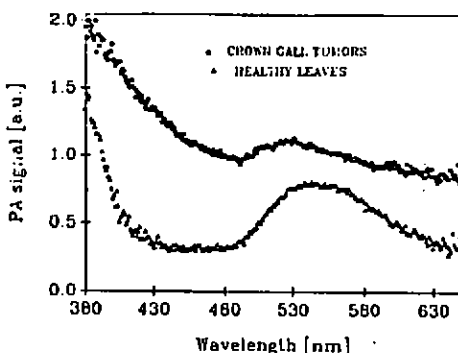


Fig. 9

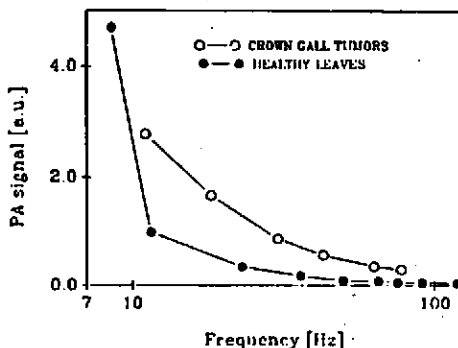


Fig. 10

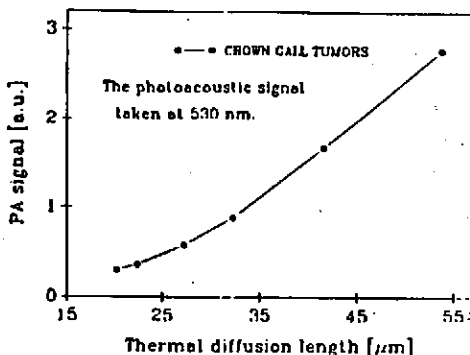


Fig. 11

PHOTOACOUSTIC EXAMINATION ...

for the two cases examined. The wave-length of light was kept constant of 530 nm. Both curves are evidently differentiated due to structural changes of the subsurface layer of the tumorous sample.

In the Fig.11 the PS signal for tumorous leaf against the thermal diffusion length is presented. The nonlinear dependence suggests appearing non-homogeneities in the structure of the upper part (deep to 30 μm) of the leaf layer.

The results presented here are interesting, however, it is difficult to establish more precise relationships between the variations in PAS observed and pathological changes of leaves structure. Anyway, the PAS spectroscopy seems to be a good tool for further examinations.

6. CONCLUSIONS

Some results of PAS examination presented in this review have shown further possibilities of the method. The selected examples of materials examined have exemplified that this non-destructive method may be used for structural interpretation and PA spectra treated as signatures of the material examined.

REFERENCES

1. R.W.B.Stephens, M.A.Ahmed, The photoacoustic effect, Proc.1-st School on Acousto-optics and Applications, Gdansk-Wiezyca, 1980, 52-68.
2. A.Rosencwaig, A.Gersho, Science 190 (1975) 556; J.App.Phys.47(1976) 64.
3. L.C.Aamodt, J.C.Murphy, J.C.Parker, J.Appl.Phys. 48(1977) 927.
4. F.A.Mc Donald, C.Wetsel, J.Appl.Phys. 49(1978) 2313.
5. A.Rosencwaig, Photoacoustic and photoacoustic spectroscopy, John Wiley & Sons, N.York, 1980.
6. T.Sawada, T.Kitamori, Analytic Applications of Photoacoustic Spectroscopy to Condensed Phase Substances, in Physical Acoustics, vol.18, Eds. W.P.Mason and R.N.Thurston, Ac.Press, 1988, 347-397.
7. J.Ranachowski, J.Rzeszotarska, J.Motylewski, E.Adamczyk, Spektroskopia fotoakustyczna w badaniach fizykochemicznych własności materiałow, in "Problemy i metody współczesnej akustyki", Ed. J.Ranachowski, PWN, Warszawa-Poznań, 1989, pp 199-210.
8. A.Sikorska, A.Sliwiński, S.Zachara, Proc.37-th Open Seminar on Acoust., Gdańsk, 1990.
9. C.J.Lewa, M.Lewa, J.Magn.Res. 89(1990) 219-226.
10. J.Szurkowski, G.Żebrowska, Zagadnienia Fizyki Współczesnej, (in print).
11. G.B.Porter, M.L.Schlafer, Ber.L.Bunsengesellschaft f.Chemie,68(1964) 316
12. J.Hamilton, I.Duncan, T.Morrow, Journ.Luminescence, 33(1985) 1.
13. G.Heinrich, M.Gusten, H.J.Ache, Appl.Spectroscopy, 40(1986) 363.
14. Cz.Lewa, Proc.ICR Spectroscopy NMR in Vivo, Lyon 1989.
15. E.H.Nagel, H.K.Lichtenthaler, in Photoacoustic and Photothermal phenomena, Eds. P.Hess, J.Pelzl, Spr.Vlg, 1988, Berlin, Heidelberg.